Advances in the analysis of thermo-active foundations

Lyesse Laloui, Thomas Mimouni and Fabrice Dupray

Laboratory of Soil Mechanics, Ecole Polytechnique Fédérale de Lausanne,

GC - Station 18, 1015 Lausanne, Switzerland.

lyesse.laloui@epfl.ch

Keywords: thermo-active foundation, geothermal pile, thermo-mechanical behaviour of soil, full scale test pile, numerical analysis, laboratory testing.

ABSTRACT

Energy geostructures are foundations equipped with absorber pipes, exchanging heat with the surrounding ground. They provide a good heat source for the heating and cooling of buildings but the temperature variations they undergo bring new challenges. Thermal expansion or contraction of the foundations can lead to building movements that must be kept within acceptable limits. Therefore, a thermo-mechanical design should be adopted. This paper presents recent advances in the understanding of the behaviour of thermo-active foundations. First, contributions of *in situ* experiments carried out on real-scale geothermal piles are reviewed. The outcome of these tests is a unique numerical design tool, called Thermo-Pile, which is presented. Next, an advanced constitutive model for environmental geomechanics accounting for non-isothermal conditions is detailed as well as the experimental evidence it was based on. Examples of thermo-hydro-mechanical analyses are presented to illustrate the challenges faced when using energy geostructures. Finally, the sustainability of heat storage through geothermal piles is assessed.

1. INTRODUCTION

Ground Source Heat Pump systems (GSHPs) have been developed in order to provide a reliable and highly efficient heat source for the heating and cooling of buildings, which represents an important part of the annual global energy demand. GSHPs take advantage of the relatively high and constant temperature levels found about 10 to 100 meters below the surface, showing coefficients of performance (COP) up to 4-5 (Brandl 2006).

GSHPs are linked to the ground through Ground Heat Exchangers (GHEs) and to the building through the heating network, forming the so-called ground source heat pump system, whose efficiency is directly linked to the efficiency of these three components.

As suggested by Brandl (2006), improving heat exchange with the ground can be achieved by embedding GHEs in foundation structures, enhancing the GHE-earth contact with the good thermal properties of concrete. Therefore, thermo-active foundations can be created from slabs, walls or deep pile foundations by inserting absorber pipes into conventional foundation structures. However, thermally activated foundations undergo thermal deformations that may compromise their primary purpose of structural support.

This paper provides insight into the advances carried out to tackle the various challenges linked to thermo-active foundations and their design.

Section 2 deals with the behaviour of geothermal piles. A major *in situ* experimental site that was developed on the EPFL campus is presented along with its main contributions to the under-standing of the thermo-mechanical behaviour of geothermal piles. The numerical tool Thermo-Pile, which was developed based on these *in situ* observations, is then described.

The thermo-mechanical behaviour of soils is detailed in Section 3. Thermo-mechanical couplings that occur in soils are then assessed with a thermo-elasto-plasticity model that was developed by our research group (ACMEG-T model). Finally, a finite element modelling of geothermal piles is presented.

2. THERMO-MECHANICAL BEHAVIOUR OF GEOTHERMAL PILES

2.1 *In situ* experiments

A geothermal test pile was installed in 1998 below a 4-storey building 100-m-long and 30-m-wide (Laloui et al. 2003).The pile is 25.8-m-long and equipped with 4 U-loops connected in parallel to head collectors. Axial deformations are monitored using strain gauges and 1-m-long optical fibres, deployed every 2 meters along the pile axis and attached to the reinforcing cage. The base reaction is measured with a load cell placed at the toe of the reinforcing cage and movements of the pile head are evaluated by 4 strain gages attached within one pile cross-section (Fig. 1). The strain gauges are equipped with thermistors for temperature correction and temperature is therefore monitored all along the pile axis. Radial expansion of the pile is monitored with optical fibres deployed around the pile perimeter at different depths (Fig. 1).

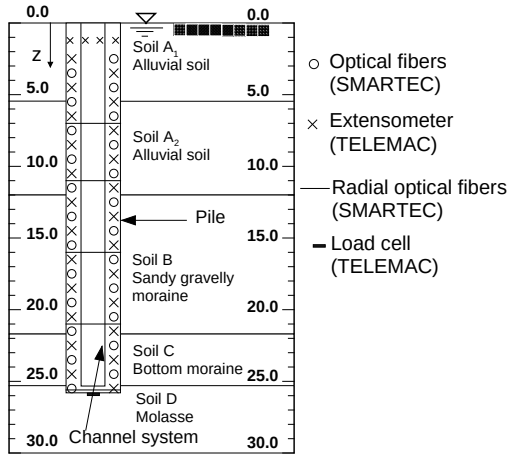

Figure 1: Stratigraphy and instrumentation of the first EPFL test pile (Laloui et al. 2003).

In this configuration, the constraints acting on the test pile is maximal as the other piles are "static" and act against its thermal deformations through raft bending. Therefore, this site gives an "upper bound" of the capping conditions that a geothermal pile could encounter below a raft.

Seven tests were carried out, following the construction stages of the building. The influence of the pile confinement on its thermo-mechanical behaviour was extensively documented and quantified by estimating the degree of freedom n (Fig. 2), defined by:

$$n = \frac{\varepsilon_{obs}}{\varepsilon_{free}} \qquad [1]$$

where ε_{obs} and ε_{free} are the measured and free axial strains. The free axial strain ε_{free} is obtained by multiplying the linear thermal expansion of the pile $\alpha_c{}^T$ by the measured temperature variation ΔT.

The degree of freedom reaches approximately 0.5 within the first 20 meters from the top of the pile at the end of the building construction (Fig. 2). This means that in this section of the pile, about half of the free thermal strain will be observed while the remaining amount will turn into internal thermal stress.

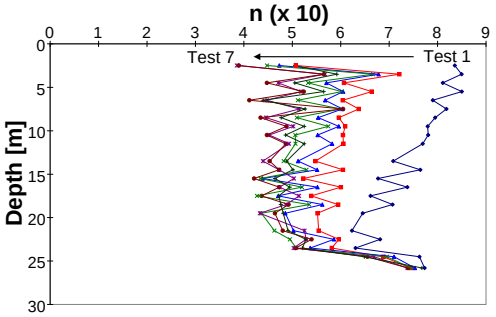

Figure 2: Evolution of the degree of freedom of the pile during the building construction (Laloui et al. 2003).

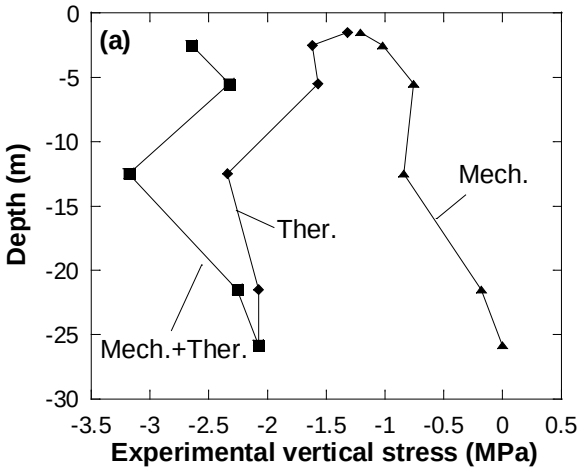

Figure 3: Vertical stress induced by mechanical and thermal loading on the first EPFL experimental pile (Laloui et al. 2003).

Finally, the variations in the internal pile load were estimated (Fig. 3); an increase of 1°C induces an internal load increase of about 100 kN (or 165 kPa).

These *in situ* experiments are a major tool for investigating the behaviour of geothermal piles and their interactions while under real service conditions.

2.2 Geotechnical design of geothermal piles

In order to include geothermal piles in project planning it is necessary to have efficient tools that can provide good estimates of the pile behaviour within a relatively short time. Currently, the use of finite element methods in engineering to assess behaviour under thermo-hydro-mechanical conditions remains limited since the method is time consuming. Therefore, there is a need to develop easy-to-use numerical tools based on simplified theories that can promote the use of geothermal piles. In this framework, we have developed a tool called Thermo-Pile that provides a simple method for estimating the thermally- induced stresses, strains and related quantities in geothermal piles (Knellwolf et al. 2011; Péron et al. 2011).

Thermo-Pile is based on the load transfer method. The load-transfer curves utilized are those proposed by Frank and Zhao (1982) and defined using an initial slope K_S and an ultimate value q_S. The slope of the linear part is related to the Menard modulus E_M. The relationships utilized in Thermo-Pile were empirically elaborated for fine-grained soils and weak rocks (FrankandZhao 1982; Amar et al. 1991):

$$K_S = \frac{2E_M}{D}; K_b = \frac{11E_M}{D} \qquad [2]$$

where K_S and K_b are the slopes used for the shaft friction and base reaction, respectively, and D is the pile diameter.

The elastic branches of the load-transfer curves are valid until the mobilized bearing capacity reaches half of its ultimate value q_s. The load-transfer curve then follows a slope equal to the fifth of the elastic slope, $K_s/5$, until the ultimate bearing capacity is reached. Unloading is achieved according to an elastic branch (Fig. 4). The ultimate bearing capacities can be user-defined or linked to soil parameters according to conventional methods (LangandHuder 1978; Legrand et al. 1993). The rigidity of the structure at the head of the pile is accounted for with a linear spring K_h. Indeed, while expanding or shrinking, the pile is pushing or pulling on the structure it is attached to (raft, beam, wall…), and thus develops a capping force.

The thermo-mechanical response of a pile is computed as follows: First, the stresses and strains induced by the mechanical loading as well as the corresponding quantities (mobilized bearing capacities, displacements) are computed using the methods described by Coyle and Reese (1966). Next, the thermal effects are estimated through an iterative process. The initialisation is achieved by assuming that the piles are totally free to move so that the initial strains are equal to the free strains and directly related to the temperature variation through the concrete thermal expansion coefficient. Next, the corresponding displacements are calculated from the null point whose displacement is, by definition, null. Then, the introduction of the estimated displacements into the load transfer curves gives a set of mobilized bearing capacity values corresponding to the internal stresses.

The thermally-induced internal stresses are related to the blocked strains so that a first set of blocked strains is estimated. Next, the blocked strains are subtracted from the previously observed strains to obtain a new strain state for the pile. This process is repeated until the desired accuracy is reached.

Thermo-Pile is currently able to perform monotonic temperature variations such as heating or cooling for one pile with a circular cross-section and embedded in a layered soil.

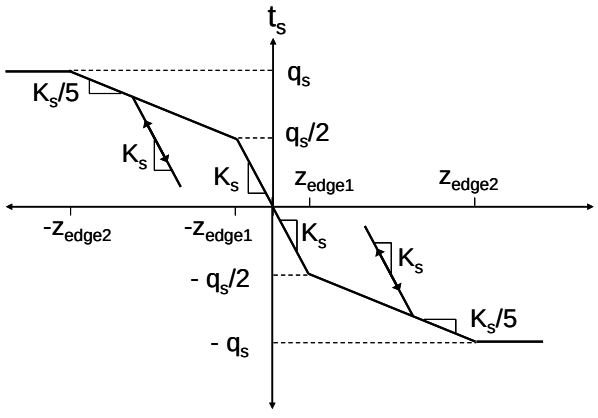

Figure 4: Example of load-transfer curve used in Thermo-Pile (Knellwolf et al. 2011).

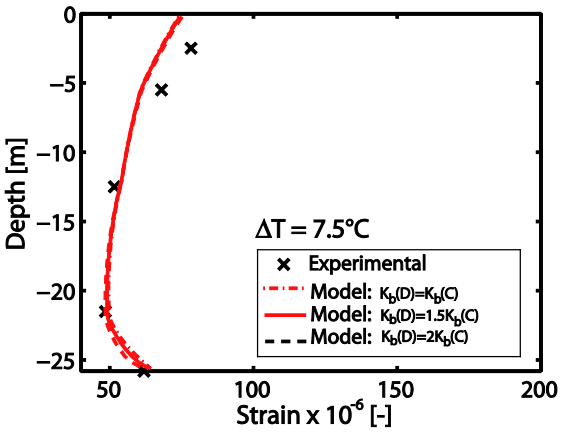

Figure 5: Example of curves used for the validation of Thermo-Pile against the first EPFL experiment (Knellwolf et al. 2011).

This tool was then validated against two major *in situ* geothermal pile experiments: the single pile test on the EPFL campus in Lausanne, Switzerland (Laloui et al. 2003) and the Lambeth college test in London, United Kingdom (Bourne-Webb et al. 2009); an ex-ample of the validation curves is shown in Fig. 5.

3. THERMO-MECHANICAL BEHAVIOUR OF SOILS

3.1. Experimental results

Temperature variation has a significant effect on the behaviour of soils. In this section, a summary of the principal experimental observations concerning thermally-induced effects on soils is given. To clarify the presentation, two types of loading paths are distinguished (Fig. 6): thermal (Path 1) and isothermal-mechanical (Path 2). Path 1 represents the behaviour of a soil subjected to a temperature variation (the difference between the present and initial or reference temperatures) at constant stress. Path 2 corresponds to mechanical loading at a given constant temperature.

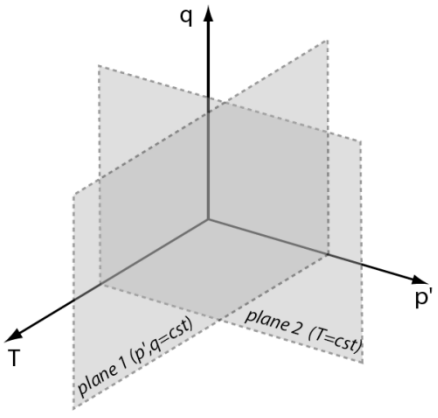

Figure 6: Thermo-mechanical loading paths; p' the effective mean pressure, q the deviatoric stress and T the temperature.

Thermal behaviour (Path 1)

Saturated soil is a two-phase material made up of a solid part (a skeleton of grains or particles surrounded by adsorbed water, for clays) and a fluid part (free water) in the inter-aggregate space (or voids).

When a soil is heated, all of the constituents dilate. In the case of clayey soils, this dilation produces a decrease in the strength of the adsorbed layers and a modification of the distance between the clay particles (Fleureau 1979). This changes the equilibrium between the Van der Waals attractive forces and the electrostatic repulsive forces, which results in one of the most characteristic thermal behaviours of clays; in normally consolidated conditions (NC), where the effect of the stress is less important (than in overconsolidated conditions (OC)), the clay contracts when it is heated and a significant part of this deformation is irreversible upon cooling. This thermal contraction is an unusual behaviour for any material. Fig. 7 illustrates the response of a sample of saturated, drained clay to a thermal heating-cooling cycle at constant isotropic stress (LalouiandCekerevac 2008).

Under heating, a NC clay sample will settle with a non-linear volume variation. Upon cooling the volume increases. The behaviour over the whole cycle indicates the irreversibility of strain due to thermal loading, which is representative of thermal hardening.

Even though there has been no physical change in the effective stresses, this behaviour can be interpreted as the soil undergoing densification, i.e. overconsolidated behaviour. The highly OC state mainly produces reversible dilation. Between these states, an intermediate one with a low overconsolidation ratio OCR, first produces dilation and then has a tendency toward contraction. The intensity of the reversible/irreversible parts of the deformations due to temperature cycling depends upon the soil type and plasticity, in addition to the stress level measured in terms of OCR. This is illustrated in Fig. 8, where the influence of OCR on the thermal behaviour of several soils is shown. It can be observed that, for a given increase in temperature, compaction is smaller for higher overconsolidation ratios and then tends to dilation.

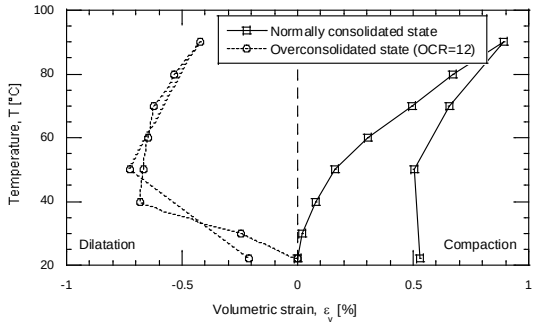

Figure 7. Thermal volumetric strains of Kaolin clay during three thermal cycles (22 °C→90 °C→22 °C) applied in NC and OC (OCR=12) states, from Laloui & Cekerevac (2008).

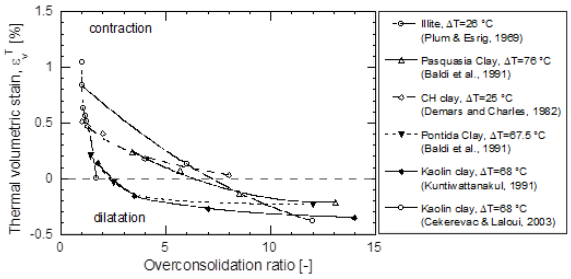

Figure 8: Influence of overconsolidation ratio on the thermal volumetric strain of clays, from Cekerevac & Laloui (2004).

Mechanical behaviour (Path 2)

Under isotropic stress conditions, the slope of the consolidation line is independent of temperature in the (*e*-ln *p'*) plane, with *e* being the void ratio and *p'* being the mean effective pressure. Experiments on saturated Illite at three different temperatures also show that heating applied prior to loading produces a densification of the sample at constant isotropic pressure (Fig. 9). To analyse the change in the preconsolidation pressure with respect to temperature, tests were conducted by heating the soil under stress loads smaller than the preconsolidation value and then applying a mechanical load under a constant temperature.

In Fig. 10 the results of tests on several clays are summarized such results for several clays (LalouiandCekerevac 2003). The pre-consolidation pressure decreases non-linearly with an increase in temperature. This decrease means that the yield limits in an isotropic plane decrease with a temperature increase. This phenomenon is independent of any viscous effects, as was shown by Boudali et al. (1994).

The thermal effect on strength is a complex process as it combines the effect of the resultant plastic strains with the intrinsic thermal one. Some experimental results are summarised in Fig. 11. A comprehensive analysis of this aspect is presented by Péron et al. (2009).

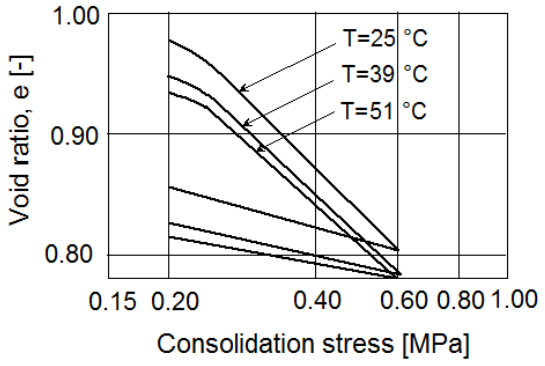

Figure 9: Isotropic consolidation of Illite samples at three different temperatures, from Campanella & Mitchell (1968).

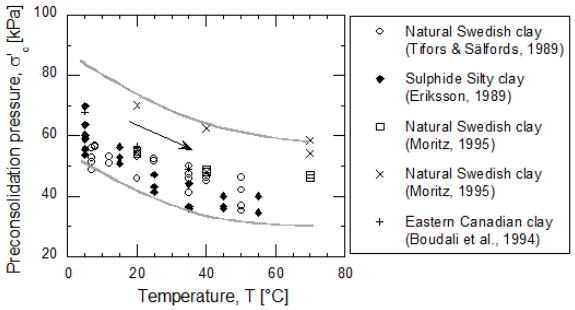

Figure 10: Influence of temperature on preconsolidation pressure from Laloui & Cekerevac (2003)

Under undrained conditions, the behaviour of the soil subjected to thermo-mechanical loading is strongly affected. Heating results in a significant pore pressure increase (PlumandEsrig 1969).

At a constant total stress difference in a triaxial test, the pore pressure growth can induce failure in the sample. Experimental results of tests on two clays reported by Hueckel & Pellegrini (1989) have shown that that clays under undrained conditions fail at temperatures of between 70°C to 90°C. It can be seen that this failure is due to an increase in pore pressure that leads to an effective main stress drop under constant total stress conditions until the critical state line is reached. The higher the initial deviatoric stress, the faster the occurrence of failure.

3.2 ACMEG-T a thermo-plastic constitutive model

The ACMEG-T model (LalouiandFrançois 2009) is developed to take into account the thermo-mechanical responses of soils observed in the previous section, and includes the thermal effects of both isotropic and deviatoric mechanisms implicated in soil plasticity. The elastoplasticity principle allows for the total strain increment, $d\varepsilon_{ij}$, to be split between thermoelastic $d\varepsilon_{ij}^{e}$ and thermoplastic $d\varepsilon_{ij}^{p}$ components:

$$d\varepsilon_{ij} = d\varepsilon_{ij}^{e} + d\varepsilon_{ij}^{p} \qquad [3]$$

The elastic part of the strain is modelled by the conventional thermo-elasticity theory (Duhamel-Neumann equation).

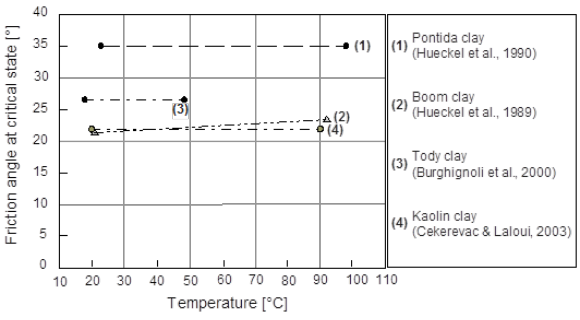

Figure 11: Effect of temperature on friction angle at Critical State from Cekerevac & Laloui (2004).

The main advantage of the present model with respect to the original isothermal model (Hujeux 1979) is the addition of non-isothermal mechanisms in the plastic component, which can be divided into an isotropic mechanism whose yield limit is f_{iso}, and a deviatoric mechanism whose yield limit is f_{dev}.

Plastic isotropic component

The yield limit f_{iso} associated with the isotropic mechanism is given by:

$$f_{iso} = p' - p_c'.r_{iso} \qquad [4]$$

where p_c' is the preconsolidation pressure and r_{iso} is the degree of plastification of the isotropic mechanisms allowing progressive evolution of the isotropic yield limit during loading and partial reversal of the limit during unloading. During loading, r_{iso} is an hyperbolic function of the plastic volumetric strain induced by the isotropic mechanism $\varepsilon_v^{p,iso}$:

$$r_{iso} = r_{iso}^{e} + \frac{\varepsilon_{\upsilon}^{p,iso}}{c + \varepsilon_{\upsilon}^{p,iso}} \qquad [5]$$

where c is a material parameter. During unloading, r_{iso} follows the decrease of the effective mean pressure, p', and at reloading, it is adjusted to keep a defined elastic nuclei (r^{e}_{iso}):

$$r_{iso} = r_{iso}^{e} + \frac{p'_{cyc}}{p_c'} + \frac{\varepsilon_{\upsilon}^{p,cyc,iso}}{c + \varepsilon_{\upsilon}^{p,cyc,iso}} \qquad [6]$$

where p'_{cyc} is the mean effective stress at the last change of direction of stress and $\varepsilon_v^{p,cyc,iso}$ is the plastic volumetric strain produced by the isotropic mechanism since the last change of direction of the stress. The preconsolidation pressure p'_c depends on the volumetric plastic strain as:

$$p_c' = p_{c0}' \exp\left(\beta \varepsilon_{\upsilon}^{p}\right) \qquad [7]$$

where β is the compressibility modulus and p'_{c0} the initial preconsolidation pressure at temperature T. The thermal effects on the yield limit are accounted for through the temperature dependency of p'_{c0} as (LalouiandCekerevac 2003):

$$p_{c0}' = p_{c0T_0}' \left(1 - \gamma_T \ln\left(\frac{T}{T_0}\right)\right) \qquad [8]$$

where p'_{c0T0} is the preconsolidation pressure at T_0 and γ_T is a material parameter. Finally, the yield limit of the isotropic mechanism is given under non-isothermal conditions by:

Laloui et al.

$$f_{iso} = p^{'} - p_{c0T_0}^{'} \exp\left\{\beta\varepsilon_v^p\right\}\left[1-\gamma_T \ln\left(\frac{T}{T_0}\right)\right] r_{iso} \quad [9]$$

Plastic deviatoric component

The yield limit associated to the deviatoric plastic mechanism is given by:

$$f_{dev} = q - Mp^{'}\left(1 - b\ln\left(\frac{p_d^{'}}{p_c^{'}}\right)\right).r_{dev} \quad [10]$$

where M is the slope of the critical state line in the *(q – p')* plane and d is the ratio between the preconsolidation pressure and the critical pressure. M is given by:

$$M = \frac{6\sin\left(\Phi^{'}\right)}{3-\sin\left(\Phi^{'}\right)} \quad [11]$$

where Φ' is the friction angle at critical state. As shown by Cekerevac & Laloui (2004) and Hueckel et al. (2011), the friction angle may depend on temperature. So, the following expression is proposed (Laloui 1993):

$$M = M_0 - g\left(T - T_0\right) \quad [12]$$

where M_0 = slope of the critical state line at ambient temperature T_0 and g = average slope of variation of friction angle at critical state with temperature.

r_{dev} can be calculated in the same way as for the isotropic mechanism, and represents the degree of plastification of the deviatoric mechanism enabling a progressive evolution of the deviatoric yield limit during loading:

$$r_{dev} = r_{dev}^e + \frac{\varepsilon_d^p}{a + \varepsilon_d^p} \quad [13]$$

where r_{dev}^e and a are material parameters defining the size of the elastic nuclei of the deviatoric mechanism and the evolution of r_{dev}, respectively, while ε_d^p is the deviatoric plastic strain.

Through a combination of the previous equations, the deviatoric yield surface becomes, under non-isothermal conditions:

Evolution of the isotropic and deviatoric yield limits with temperature are shown in Fig. 12. Validations of the model against laboratory tests can be found in (LalouiandFrançois 2009).

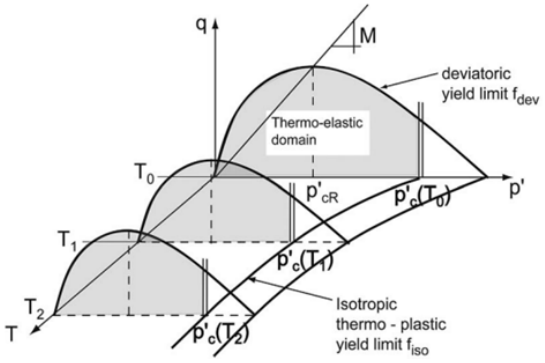

Figure 12: Coupled thermoplasticity yield limits (LalouiandFrançois 2009)

$$f_{dev} = q - r_{dev}p^{'}\left[M_0 - g\left(T-T_0\right)\right]* \left\{1 - n\ln\left(\frac{dp^{'}}{p_{c0T_0}^{'}\exp\left\{\beta\varepsilon_v^p\right\}\left[1-\gamma_T\ln\left(\frac{T}{T_0}\right)\right]}\right)\right\} = 0 \quad [14]$$

3.3 Example of numerical modelling of geothermal structures

3.3.1 Identification of the thermo-mechanical behaviour of a heat-exchanger foundation

The structure under consideration

In the previous sections, the thermo-mechanical behaviour of a single isolated geothermal pile is studied experimentally and the thermo-mechanical characteristics of the soil are presented from both experimental and constitutive modelling points of view. In order to gain a global understanding of the system it is necessary to simulate the response of a foundation from both thermal and mechanical perspectives.

In this section, the behaviour of a multi-pile heat exchanger foundation subjected to thermo-mechanical loading is examined numerically from both thermal and mechanical perspectives.

A 2D-approach is used for this purpose. For satisfactory seasonal storage performance, a large reservoir is required (greater than 30 000 m^3, according to Pahud (2002)). For a conventional building in dense clayey soil, the typical pile length is 20 m. Because the system is analysed in 2D, the volume is "infinite", but for the purpose of using realistic numbers, it has been decided to use a theoretical storage volume of 104'000 m^3. This foundation, shown in Fig. 13, would consist of 105 piles (7x15), each with a diameter of 80 cm and a length of 20 meters, spaced 7 meters apart in a square pattern. The foundation is considered to function as a piled raft and is located on deep, low-permeability, clayey soil, which is assumed to be homogeneous and to behave thermo-elastically in the range of temperatures considered.

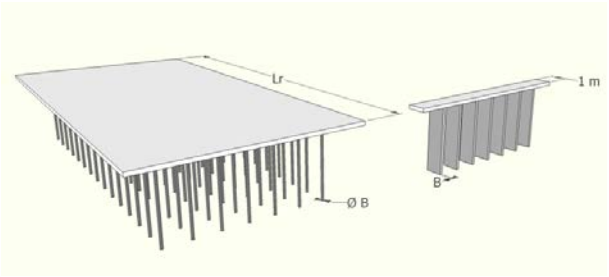

Figure 13: 3D foundation and representation of the equivalent 2D foundation

Interactions between the thermal, mechanical and hydraulic responses are the main source of uncertainty in the design of a thermal energy storage geostructure. Heat exchange is the driving physical factor in this problem, and it creates thermal strains and thermal diffusion. As such, heat exchange also has hydraulic and mechanical consequences.

The numerical simulations are run using the FEM code *Lagamine* (Charlier 1987; Collin et al. 2002). The finite element mesh (Fig. 14) is composed of 3863 nodes and 1240 8-node elements.

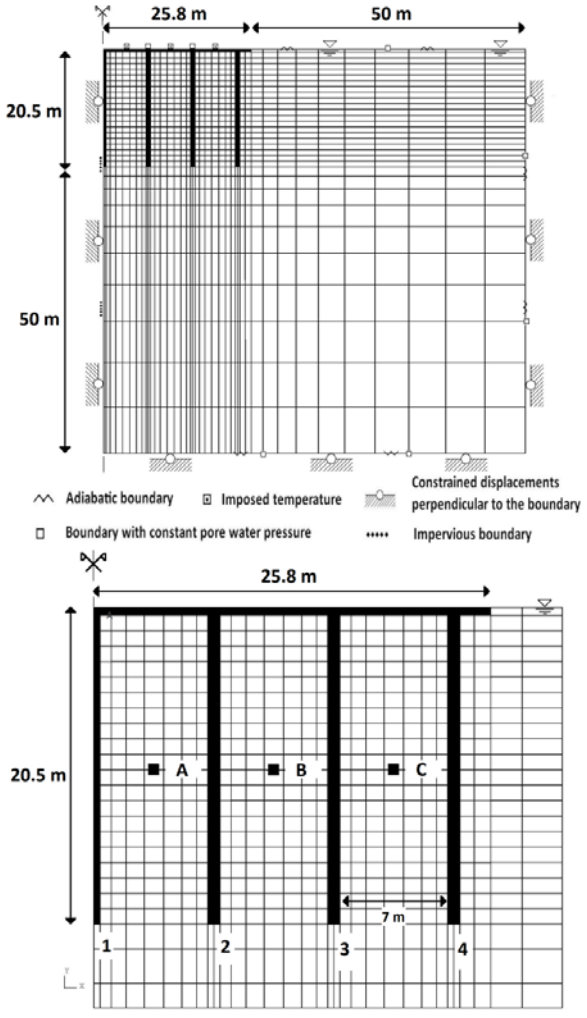

Figure 14: Pile foundation configuration and FE mesh

Concepts for the transition from a 3D to a 2D configuration

From a mechanical point of view, the transition from 3D to 2D for a piled raft foundation can be considered by modifying the Young's modulus of the piles, as indicated in Prakoso and Kulhawy (2001). The responses of vertically loaded pile foundations are controlled primarily by the axial stiffness of the piles. Because the piles are simplified into strips in a plane, a row of piles has to be simplified into an equivalent plane strain pile with the following modified Young's modulus:

$$E_{eq} = \frac{n_{p-row} A_p}{L_r B} E_p = e_{eq} E_p \qquad [15]$$

where E_{eq} is the equivalent elastic modulus, E_p is the concrete elastic modulus, A_p is the pile section, B is the pile diameter, L_r is the slab length (in plane), $n_{p\text{-}row}$ is the number of piles in a row, and e_{eq} is the 3D-2D coefficient, as defined in equation [15].

An extension of this principle to thermo-hydro-mechanical conditions has been proposed by Dupray et al. (2013), which makes use of the effective stress framework to determine the correct representation of the pile behaviour in this 2D situation.

The effect of water pressure on the actual stresses should be written as follows:

$$\sigma'_p = \sigma_p - p_w \mathrm{I} = \frac{E_{eq} \varepsilon^e}{e_{eq}} \qquad [16]$$

where p_w is the pore water pressure and $\boldsymbol{\sigma}'_{\mathbf{p}}$ is the real effective stress in the pile. This is also written as the first line of the following set of equations, while the second line simply uses the general form of the effective stress definition, with $\boldsymbol{\sigma}_{\mathbf{eq}}$ and c as unknowns:

$$\begin{cases} e_{\mathbf{eq}} \boldsymbol{\sigma}'_p = e_{\mathbf{eq}} \boldsymbol{\sigma}_p - e_{eq} \times p_w \mathbf{I} \\ \boldsymbol{\sigma}'_{\mathbf{eq}} = \boldsymbol{\sigma}_{\mathbf{eq}} - c \times p_w \mathbf{I} \end{cases} \qquad [17]$$

As the strains of the real and equivalent material are assumed to be equal, the left terms are equal, leading to the solution:

$$\begin{cases} \boldsymbol{\sigma}_{\mathbf{eq}} = e_{eq} \boldsymbol{\sigma}_{\mathbf{p}} \\ c = e_{eq} \end{cases} \qquad [18]$$

Thermal strains in the pile are also affected by its representation as a wall. Thermal expansion in the out-of-plane direction is blocked while it would be almost free in a pile. The thermal expansion coefficient used in the model is therefore reduced to compensate the increase by a factor (1+ ν) of the axial thermal expansion, as calculated in plane-strain thermo-elasticity.

The transition from 3D to 2D simulation also has consequences for the thermal aspect of the problem. The choice is made to inject and extract from the corresponding "wall" the same amount of energy as in the piles. This assumption leads to a different repartition of temperature in the vicinity of the piles because this energy is transferred to the soil over a larger surface than in reality. It is also more appropriate in the long term because both the heat storage ground volume and the energy exchange are equal to the real values.

General THM formulation

The diffusive model that is used in this simulation was written and implemented in the software used by Collin (2003). Only a short description of the principles of the approach is presented here. The equilibrium and balance equations, as well as the water and heat flows, are expressed in the moving current configuration through a Lagrangian-updated formulation.

Table 1: Thermal, hydraulic and mechanical characteristics of clayey soil and concrete

	Clayey soil
Porosity n	0.39
Intrinsic permeability	1×10^{-14} m^2
Solid thermal conductivity λ_s	2.42 W.m^{-1}.K^{-1}
Solid specific heat $c_{p,s}$	732 J.kg^{-1}.K^{-1}
Solid specific mass ρ_s	2 700 kg.m^{-3}
Elastic modulus	100 MPa
Poisson's coefficient	0.3
Volumetric thermal expansion coef.	1.2×10^{-4} K^{-1}
	Concrete (piles and slab)
Porosity n	0.12
Intrinsic permeability	1×10^{-16} m^2
Solid thermal conductivity λ_s	1.7 W.m^{-1}.K^{-1}
Solid specific heat $c_{p,s}$	880 J.kg^{-1}.K^{-1}
Solid specific mass ρ_s	2 300 kg.m^{-3}
Elastic modulus	35 000 MPa
Poisson's coefficient	0.25
Volumetric thermal expansion coef.	3.6×10^{-5} K^{-1}
3D-2D equivalent coefficient	0.089
Equivalent elastic modulus	3 125 MPa
	Water
Dynamic viscosity	$f(T)$
Compressibility	4.54×10^{-10} Pa^{-1}
Volumetric thermal expansion coef.	2.1×10^{-4} K^{-1}
Water thermal conductivity λ_w	0.57 W.m^{-1}.K^{-1}
Water specific heat $c_{p,w}$	4186 J.kg^{-1}.K^{-1}
Water specific mass ρ_w	1 000 kg.m^{-3}

The model uses a phenomenological description that averages properties of the medium (enthalpy, conductivity) depending on the spatial repartition of its constituents. Water is considered to be compressible and soil grains incompressible but both are affected by thermal dilation. The properties of the soil and concrete are presented in Table 2.

3.3.2 Boundary conditions and initial configuration

It is assumed that the energy geostructure under consideration does have any similar structures nearby. As a consequence, a constant temperature is imposed on the lower and lateral boundaries of the mesh, which are at a distance from the heated volume. The axis of symmetry is naturally an adiabatic boundary. The initial temperature of the ground is fixed at 11 °C, which is a typical value in temperate regions. A temperature of 15 °C is applied at the slab nodes to account for the presence of the thermally controlled building. No exchange of water or heat is considered between the soil surface and the environment. With respect to the mechanical boundary conditions, restrictions are applied to both the vertical and horizontal displacements at the base of the mesh and to the horizontal displacements on the sides of the mesh. The size of the model ensures that the outer boundaries are sufficiently far from the building. The initial stresses in the model due to gravity are introduced by assuming a coefficient of earth pressure at rest of $K_0=0.5$.

The initial pore water pressure corresponds to the hydrostatic profile with a water table located at the surface. Because of the assumption of saturated conditions, the water table remains at the top of the model during the simulation.

Loading path

An evaluation of the bearing capacity of the structure was conducted according to the norm SIA-267 (2003) with assumed frictional parameters. Based on this norm, it was decided to apply a mechanical loading of 1500 kN on each pile, which corresponds to a 3 MPa stress on an isolated pile. The first step consists in applying this load on top of the simulated piles, through the raft. Sufficient time is given to allow dissipation of additional pore pressure.

Thermal loading is then applied and cycled for five years. The thermal load is applied directly to the piles in the form of a uniform surface source/sink term. Heat injection and extraction rates are estimated based on the most efficient systems in service today, and higher rates are also studied because they offer better volumetric efficiency. Nevertheless, sustainability and reload during the non-heating period should be ensured (Choi et al. 2011).

In the simulation, the heat extraction and injection rates are fixed at 90 W/m at the beginning (scenario 1, shown in Fig. 15 along with other scenarios).

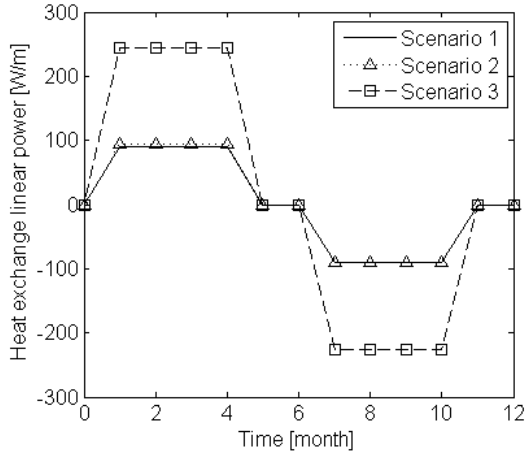

Figure 15: Loading functions as imposed on the piles

For comparison, in the high-rise building "Palais Quartier" in Frankfurt, a total heating and cooling power of nearly 1 000 kW is made available by the use of 392 thermo-piles, each measuring 30 m (Katzenbach et al. 2009). This power corresponds to a heating and cooling injection rate of approximately 84 W/m.

These profiles do not take into account daily variations. Heat storage comes first with a linear increase, as would happen in May, setting day zero. Scenario 2 is used to evaluate the thermal losses, while scenario 3 aims at representing future improvements in the availability of warmer heat sources such as solar thermal panels. Heat exchange is dissipated uniformly on the cross-section of the pile.

3.3.3 Thermal results

In the reference scenario, the injection and extraction rates are 90 W/m. The total input and output are therefore 1960 GJ, or considering the theoretical size of the system, 18 MJ/m^3 on average, corresponding to a mean temperature difference in the soil of 4.7 °C. In order to precisely characterise the temperature evolution in the storage system, node C is monitored (Fig. 14). This node is located at a depth of 10 m beneath the slab and is equidistant between piles 3 and 4. It corresponds to a zone closer to the edge of the storage system, where losses are more visible while still being clearly within the storage zone. Fig. 16 shows the evolution of temperature at point C over time, and the temperature change of 5.1 °C in scenario 1 indicates that point C is a good overall indicator of the mean storage temperature. In general, the temperature in the storage zone varies between 6 °C and 21 °C during a cycle. The temperature in this case is clearly decreasing slightly, indicating that thermal losses are present but of a low magnitude. Scenario 2 serves to quantify these losses, setting the injected heat at such a rate that temperatures in the heat store evolve in a permanent regime over the years. This is achieved by injecting 95 W/m instead of 90 W/m, or 5.5 % heat loss per year, in the cross-section.

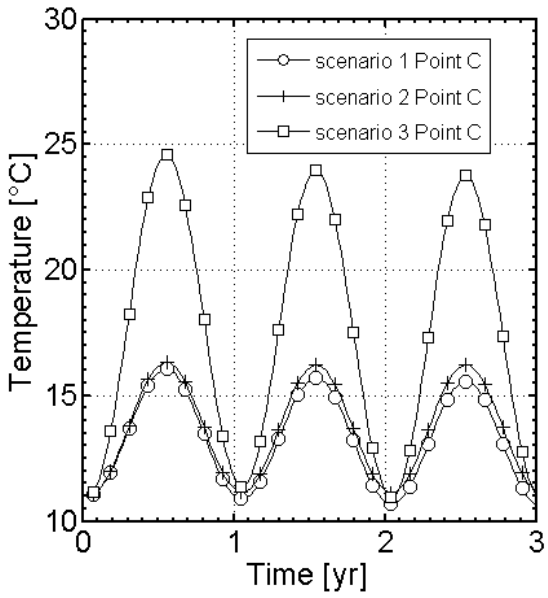

Figure 16: Evolution of the temperature in the storage system over three years for various injection/extraction ratios.

Doubling the losses because of the 3D effect leads to an efficiency (ratio of extracted heat to injected heat) of 0.89, close to the one (0.85) observed by Lund and Östman (1985) in a non-structural system.

An increase in the heat exchange rate is shown in scenario 3, with an extraction rate of 225 W/m and an injection rate of 245 W/m. In line with expectations, this turns into an increase of the average storage temperature and therefore into higher losses, with the efficiency reaching 0.83.

3.3.4 Mechanical implications

Several experimental studies have been performed that provide information about the mechanical response of a single pile when thermally loaded. The main results are from data obtained from the EPFL test pile (Laloui et al. 2003) and the Lambeth College test pile (Bourne-Webb et al. 2009). These studies have enabled the calculation of a range of pile stresses that can be created by thermal loading, the maximum varying between 100 and 192 kPa/°C (Amatya et al. 2012).

The differences seen between a single geothermal pile and a whole foundation are investigated in this section. In order to do so, the case where the whole foundation is used as heat-exchanger is compared to the situation where only one row of piles (the central one) is used for heat exchange.

For the reference scenario (90 W/m), the increase in temperature in the piles is in line with the previously mentioned experiments, at 10°C. In contrast to the single pile experiments, the additional stress due to temperature is very limited, reaching 0.325 MPa (see Fig. 17) which is less than 10 % of the design stress.

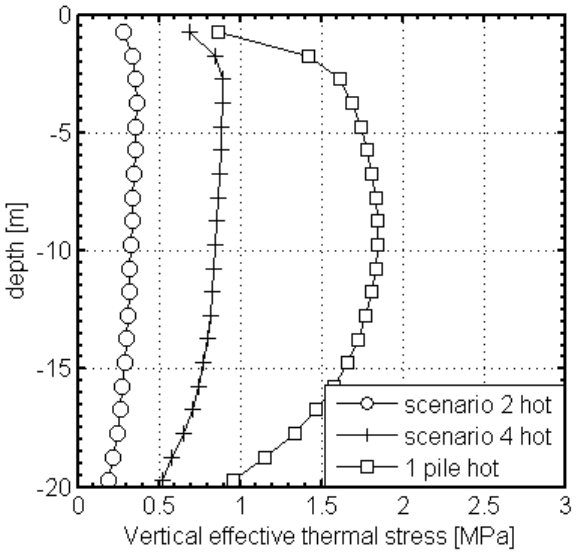

Figure 17: Vertical stress induced by constrained thermal strains in the first pile.

This stress only amounts to 25 kPa/°C (primarily due to the group effect), as will be discussed in the next section. For the extraction period, the behaviour is slightly different because the stress reduction appears to be slightly more dependent on temperature, reaching 50 kPa/°C.

In the range of temperature considered, it is estimated that, for an injection rate of 90 W/m in a homogeneously used geostructure, the maximum effect of temperature on the pile stress should not change the design principles of such a foundation. These effects may be taken into account either through evaluation, such as in this simulation, or through an additional safety coefficient. To explore the limits of acceptable temperature increase from this point of view, simulations with higher rates of injection and extraction have been run. Thermal scenario 3, in which the temperature in the piles evolves between 1 and 35 °C, is used for this purpose. The maximal thermal overstress value observed is equal to 0.63 MPa, which represents 21 % of the total mechanical loading. The additional stress in this case is 26 kPa/°C, which is similar to the value found at lower temperatures.

When considering only one row of piles for heat exchange, the maximum thermal overstress value becomes equal to 1.4 MPa, or 50% of the mechanical loading, and 62 kPa/°C, which is slightly lower than the previously identified values which were in the range of 100 kPa/°C (obtained in very different conditions). The partial use of a foundation as a heat exchanger introduces significant stresses due to the stiffness of the rest of the geostructure. This scenario can and should be avoided by the whole foundation as a heat exchanger.

4. CONCLUSIONS

The first thermo-active test pile built on the EPFL campus allowed the load-transfer mechanism under temperature changes to be observed as well as the influence of the pile head load on the pile confinement. It was observed that the free thermal strain was split into real thermal strains measured using embedded strain gauges while the remaining part was turned into internal thermal stress. The mechanical state of the pile after any temperature change is relevant for maintaining equilibrium between the thermal strains and stresses and is strongly dependent on the surrounding stratigraphy and building characteristics.

A design tool, Thermo-Pile, was developed based on results obtained from the first experimental site at EPFL as well as the Lambeth College test pile. This tool was shown to be capable of reproducing the stress and strain states of geothermal piles under given temperature changes.

Next, the thermo-mechanical behaviour of soils was assessed. A thermo-elasto-plastic model, ACMEG-T which was developed based on the experimental results, is described. The thermal effects on the soil response are quantified as a variation of the preconsolidation stress, which decreases with temperature.

Examples of thermo-hydro-mechanical analyses are given. The behaviour of a piled raft is investigated. Group effects are quantified by comparing the induced stresses in piles when only one pile is heated and when the whole foundation is heated. It is shown that heating the whole assemblage of piles induces lower stresses in the reference pile as the whole raft heaves. Conversely, heating a single pile maximizes its confinement by the raft so that thermal stresses increase.

The variety of the recent developments in research about energy geostructures cater to every need, from the engineer tasked with designing one, to future developments in the understanding of long-term challenges. The overview proposed in this article also highlights the maturity of the topic, making it suitable for going forward with design regulations that would help promote the technology.

5. ACKNOWLEDGEMENTS

The authors thank EOS Holding for its financial supports through the project GRETEL for the numerical analyses of piled rafts with geothermal piles.

The support of the Swiss Federal Office of Energy (OFEN) for the *in situ* test was much appreciated (project N° 25483).

REFERENCES

Amar S., Clarke B. G. F., Gambin M. P. and Orr T. L. L.: The application of pressuremeter test results to

foundation desing in Europe, Part 1: Predrilled pressuremeters - selt-boring pressurementers., European Soil Mechanics and Foundation Engineering. European Regional Technical Committee N°. 4. A. A. Balkema, Rotterdam, The Netherlands, (1991).

Amatya B., Soga K., Bourne-Webb P. J., Amis T. and Laloui L.: Thermo-mechanical Behaviour of Energy Piles, *Géotechnique*, **62**(6), (2012), 503-519.

Boudali M., Leroueil S. and Sinivasa Murthy B. R.: Viscous behaviour of natural clays, 13th International Conference on Soil Mechanics and Foundation Engineering, New Delhi, India, (Year),

Bourne-Webb P. J., Amatya B., Soga K., Amis T., Davidson C. and Payne P.: Energy pile test at Lambeth College, London: geotechnical and thermodynamic aspects of pile response to heat cycles, *Géotechnique*, **59**(3), (2009), 237-248.

Brandl H.: Energy foundations and other thermo-active ground structures, *Geotechnique*, **56**(2), (2006), 81-122.

Campanella R. G. and Mitchell J. K.: Influence of temperature variations on soil behavior, *Journal of soil Mechanics & Foundations Division ASCE*, **94**(SM3), (1968), 709-734.

Cekerevac C. and Laloui L.: Experimental study of thermal effects on the mechanical behaviour of a clay, *International Journal for Numerical and Analytical Methods in Geomechanics*, **28**(3), (2004), 209-228.

Charlier R.: Approche unifiée de quelques problèmes non linéaires de mécanique des milieux continus par la méthode des éléments finis. Ph.D. Thesis, Université de Liège, Liège, Belgium, (1987).

Choi J. C., Lee S. R. and Lee D. S.: Numerical simulation of vertical ground heat exchangers: Intermittent operation in unsaturated soil conditions, *Computers and Geotechnics*, **38**(8), (2011), 949-958.

Collin F., Li X., Radu J. P. and Charlier R.: Thermo-hydro-mechanical coupling in clay barriers, *Engineering Geology*, **64**((2002), 179-193.

Collin F.: Couplages thermo-hydro-mécaniques dans les sols et les roches tendres partiellement saturés. Ph.D. Thesis, Faculté des Sciences Appliquées, Université de Liège, Liège, Belgique, (2003).

Coyle H. M. and Reese L. C.: Load transfer for axially loaded piles in clay., *Journal of the Soil Mechanics and Foundations Division*, **92**(2), (1966), 1-26.

Dupray F., Laloui L. and Kazangba A.: Numerical analysis of seasonal heat storage in an energy pile foundation, *Computers and Geotechnics*, **(in revision)**((2013),

Fleureau J. M.: Influence d'un champ thermique ou électirque sur les phénomènes d'interaction solide-liquide dans les milieux poreux. Ph.D. Thesis, Ecole Central de Paris, Paris, France, (1979).

Frank R. and Zhao S. R.: Estimation par les paramètres pressiométriques de l'enfoncement sous charge axiale de pieux forés dans des sols fins., *Bull Liaison Lab Ponts Chaussées*, **119**((1982), 17-24.

Hueckel T. and Pelligrini R. (1989). Modeling of thermal failure of saturated clays. International Symposium on Numerical Models in Geomechanics. NUMOG**:** 81-90.

Hueckel T., François B. and Laloui L.: Temperature-depedent internal friction of clay in a cylindrical heat source problem, *Géotechnique*, **61**(10), (2011), 831-844.

Hujeux J. C.: Calcul nemérique de problèmes de consolidation élastoplastique. Ph.D. Thesis, Ecole Centrale de Paris, Paris, France, (1979).

Katzenbach R., Ramm H. and Waberseck T. (2009). Recent developments in foundation and geothermal engineering. 2nd International Conference on New Developments in Soil Mechanics and Geotechnical Engineering. Near East University, Nicosia, North Cyprus.

Knellwolf C., Péron H. and Laloui L.: Geotechnical analysis of heat exchanger piles, *Journal of Geotechnical and Geoenvironmental Engineering*, **137**(10), (2011), 890-902.

Laloui L.: Modélisation du comportement thermo-hydro-mécanique des milieux poreux anélastiques. Ph.D Thesis, Ecole Centrale de Paris, Paris, France, (1993).

Laloui L. and Cekerevac C.: Thermo-plasticity of clays: An isotropic yield mechanism, *Computers and Geotechnics*, **30**(8), (2003), 649-660.

Laloui L., Moreni M. and Vulliet L.: Comportement d'un pieu bi-fonction, fondation et échangeur de chaleur, *Canadian Geotechnical Journal*, **40**(2), (2003), 388-402.

Laloui L. and Cekerevac C.: Non-isothermal plasticiy model for cyclic behaviour of soils, *International Journal for Numerical and Analytical Methods in Geomechanics*, **32**((2008), 437-460.

Laloui L. and François B.: ACMEG-T: Soil thermoplasticity model, *Journal of Engineering Mechanics*, **135**(9), (2009), 932-944.

Lang H. J. and Huder J.: Bodenmechanik und Grundbau: Das Verhalten von Böden und die wichtigsten grundbaulichen Konzepte., (1978).

Legrand J., Millan A. and Renault J.: Règles techniques de conception et de calcul des fondations des ouvrages de génie civil., Fascicule N° 62, Titre V, M. d. l. é. d. l. e. d. transports, France, (1993).

Lund P. D. and Östman M. B.: A numerical model for seasonal storage of solar heat in the ground by vertical pipes, *Solar Energy*, **34**(4-5), (1985), 351-366.

Pahud D.: Geothermal energy and heat storage, SUPSI Laboratorio di Energia, Ecologia ed Economia. Lugano, Switzerland, (2002).

Peron H., Hueckel T., Laloui L. and Hu L. B.: Fundamentals of desiccation cracking of fine-grained soils: experimental characterisation and mechanisms identification, *Canadian Geotechnical Journal*, **46**(10), (2009), 1177-1201.

Péron H., Knellwolf C. and Laloui L.: A method for the geotechnical design of heat exchanger piles., Geo-Frontiers 2011 Conference, ASCE, Dallas, Texas, USA, (Year), 470-479.

Plum L. and Esrig M. I.: Some temperature effects on soil compressibility and pore water pressure, Highway Research Board. Special report, Report 103. Washington, USA., (1969).

Prakoso W. A. and Kulhawy F. H.: Cointribution to piled raft foundation design, *Journal of Geotechnical and Geoenvironmental Engineering*, **127**(1), (2001), 17-24.

SIA-267: Géotechnique. Société suisse des ingénieurs et des architèctes, (2003).